Rod-Coil Copolymers: Their Aggregation Behavior

A. Halperin

The Fritz Haber Research Center for Molecular Dynamics, The Hebrew University, Jerusalem 91904, Israel

Received August 16, 1989; Revised Manuscript Received November 3, 1989

ABSTRACT: The aggregation behavior of rod-coil block copolymers in a selective solvent of low molecular weight is considered within the scaling approach. The equilibrium structure of micelles and lamellae is analyzed. Thermodynamically stable micelles are characterized by extended, starlike coronas. The lamellae are expected to exhibit a tilting, smectic A-smectic C, first-order phase transition driven by the competition between surface and deformation free energies. The Petschek-Wiefling design for ferroelectric smectic phases is analyzed in the case of swollen lamellar phases formed by ABC coil-rod-coil copolymers. The alignment of the electrical dipoles is pictured as a result of the interaction between "chemical dipoles". A novel application of this scheme to the design of paraelectric, optically active micelles is considered.

I. Introduction

The study of block copolymers tends to focus on flexible chains. Less is known of the behavior of block copolymers incorporating rigid, rodlike blocks (Figure 1). This is particularly true with regard to the *aggregation behavior of such rod-coil copolymers in selective solvents*, that is, solvents in which the rodlike blocks are immiscible while the flexible blocks are highly soluble. This problem is of interest to liquid crystals research as well as to polymer and surface science. Rod-coil copolymers provide an attractive model system for the study of liquid crystals. Smectic, layered, liquid crystals are frequently formed by low molecular weight moieties consisting of a rigid cylindrical core attached to a flexible tail or two.[1] Accordingly, rod-coil block copolymers are the macromolecular analogues for "monomeric" smectogens.[2] As model smectogens, rod-coil copolymers afford the characteristic polymeric advantages: (i) a simpler theoretical description in terms of asymptotic properties; (ii) the option to vary the size of the constituting blocks over a wide range and to study the ensuing trends. Another attractive feature is their capability of forming smectic phases in melt as well as in solution.[2,3] This trait sets them apart from both monomeric, thermotropic smectogens and low molecular weight surfactants. Typically, members of the first category do not form liquid crystals in solution while those of the second group form mesophases only in the presence of a selective solvent.[4] Rod-coil copolymers are both thermotropic smectogens and polymeric surfactants. This is a useful attribute as it allows one to study smectic phases as the amount of solvent in the sample is continuously varied. In particular, the diluent content adjusts the separation between smectic layers, thus modifying their coupling.[5] The solvent also makes for better viscosity control, an important consideration for polymeric liquid crystals. Apart from the points considered above, ABC coil-rod-coil triblock copolymers provide a promising starting point for the design of ferroelectric liquid crystals: The design, suggested by Petschek and Wiefling,[6] utilizes the incompatibility of the A and C blocks to align the dipoles associated with the rigid B segments. Finally, rod-coil copolymers are also polymeric amphiphiles. In turn, the aggregation behavior of polymeric surfactants is of current interest in both surface[7] and polymer science.[8] Exploration of the differences between the aggregation behavior of coil-coil and rod-coil copolymers is expected to add to our understanding of these phenomena.

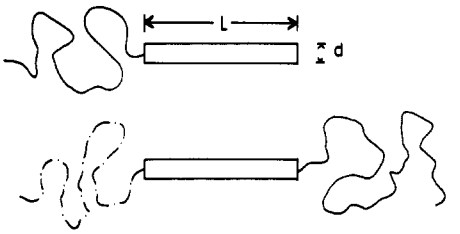

Figure 1. Two types of block copolymers considered in this paper: (a) AB coil-rod diblock copolymers and (b) ABC (or ABA) coil-rod-coil triblock copolymers.

Before we turn to the distinguishing features of rod-coil aggregates, it is helpful to list certain traits common to both systems.[8] In all such aggregates one may distinguish two regions: an inner core consisting of the immiscible blocks and an outer corona comprising soluble blocks swollen by the solvent.[9] The precise geometry of the two regions depends on the nature of the aggregates (micelles, lamellae, etc.) and the copolymer type (coil-coil or rod-coil). Yet, in all cases the blocks' junctions are constrained to the core-corona interface. Accordingly, both core and coronal blocks are, in effect, grafted to the core-corona boundary, i.e., attached to the interface by a single "head group". This is a crucial point as densely grafted flexible chains are strongly deformed.[8,10] In turn, the associated free-energy penalty plays an important role in determining the aggregates' equilibrium structure. Finally, the aggregation, in both systems, is driven by the surface free energy of the core-corona boundary: The number of unfavorable contacts between the solvent and the immiscible blocks is lowered when assemblies are formed. Clearly, the differences between the two systems are traceable to the core structure. The core of coil-coil aggregates is commonly pictured as a melt of the immiscible blocks. The constant density constraint on the grafted core blocks requires chain deformation. This is most clearly seen in micelles. When the core's radius is large in comparison to the size of an ideal coil, it is necessary to stretch some blocks in order to "fill" the core's center. This deformation gives rise to a free-energy penalty favoring smaller micelles. A different core structure is expected in aggregates of rod-coil copolymers: (i) The configuration of a rigid, rodlike block is, by definition, unique. No configurational changes are thus expected upon aggregation. As a result, there is no free-energy penalty due to the deformation of core blocks in rod-coil aggregates. Their growth is arrested by the

0024-9297/90/2223-2724$02.50/0

penalty associated with the stretching of the coronal chains. (ii) Aggregated rods are expected to favor ordered packing with their long axes aligned. This mode is markedly different from the meltlike state of flexible core blocks. The geometry of rod-coil assemblies is accordingly different. For example, micelles formed by coil-coil copolymers are known to have spherical cores while micelles consisting of rod-coil copolymers are expected to have cylindrical cores. In turn, this distinction is reflected in the scaling behavior of the core's surface area and the associated free energy.

In the following we aim to make the above observations more quantitative. Initially we present theoretical considerations pertaining to the aggregation behavior of rod (B)-coil (A) diblock copolymers. However, the scaling behavior found for aggregated AB copolymers is expected to hold for aggregates of ABA coil-rod-coil copolymers providing the A blocks are of equal size. We consider the equilibrium structure of micelles and lamellae formed by monodispersed, *neutral*, AB copolymers consisting of N_A A monomers and N_B B monomers. In particular, we focus on their aggregation behavior in selective solvents of *low molecular weight*: a nonsolvent for the rodlike B blocks but a good solvent for the flexible A blocks. Initially the copolymers are assumed to have no electrical dipoles. Electrical dipoles are introduced later, in our discussion of the ABC coil-rod-coil assemblies and the Petschek-Wiefling scheme for ferroelectric design.[6] The equilibrium structure of rod-coil micelles is considered in section II. The analysis indicates that stable micelles are endowed with extended, starlike coronas. The important variable in this section is the mean aggregation number. Section III deals with the structure of nonoverlapping sheets in a swollen lamellar phase formed by rod-coil copolymers. Here, the main issue is the role of rod tilt in the relief of A coil deformation. The competition between surface and deformation free energies gives rise to a first-order, smectic A-smectic C, phase transition in the lamellae. Micelles and lamellae of ABC coil-rod-coil copolymers are considered in section VI. Only copolymers having flexible blocks of equal size ($N_A = N_C$) are considered. In this case the B blocks carry electric dipoles. Our concern is with the utilization of the Petschek-Wiefling scheme for the design of paraelectric micelles. In all cases we analyze the structure of a single, noninteracting, aggregate, assuming that the diblock copolymers are completely insoluble in the solvent; i.e., the equilibrium structure corresponds to a minimum in the free energy per aggregated chain.[11] In particular, electrical interactions between different aggregates are overlooked in section VI. For simplicity we ignore the effect of van der Waals interactions on the system. The discussion is based on scaling arguments. As is customary in scaling analysis, numerical prefactors are omitted.

II. Mainly on Micelles

In the simplest model for the core of rod-coil micelles, the B rods form a right circular cylinder or disk of radius R_{core} (Figure 2). It is assumed that the rods' long axes are aligned and their tips toe the basal plane. In general, one must allow for rod tilt with respect to the core's axis. However, as we shall see, this effect is not significant for micelles. The rods are thus assumed to align with the core axis. The physical justification for this model is that it clearly achieves a minimum in the core's surface free energy. We further assume that the highly selective solvent is excluded from the core; i.e., $\phi_B \approx 1$. For a micelle consisting of f copolymers, the core's volume

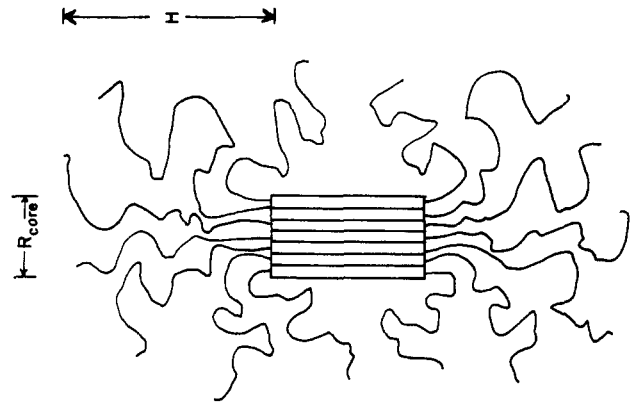

Figure 2. Schematic cross section of a micelle formed by AB coil-rod copolymers. The core, of radius R_{core} and height L, consists of f immiscible aligned rods. The double corona comprises two extended, starlike coronal "mops" of radius H.

scales as fLd^2 where L is the rod's length and d is its diameter. The height of the cylindrical core is L while its radius is $R_{core} \sim f^{1/2}d$. Upon designating the core's "surface tension" by γ, its surface free energy per chain is given by

$$F_{interface}/kT \sim (\gamma d^2/kT)(1 + f^{-1/2}L/d) \quad \text{(II.1)}$$

As noted earlier, the coronal coils are, in effect, grafted to the core's two basal plates, forming two coronal "mops". The average separation of grafting sites, assuming random distribution among the two bases, is d. It is now possible to distinguish two extreme cases: (i) The thickness, H, of the coronal layer is much larger than R_{core}. In this limit the coronas adopt a starlike structure.[12,13] The coronas are essentially spherical, and the cylindrical core acts as a weak perturbation to the starlike mops (Figure 2). The Daoud-Cotton model[14] provides a convenient description for such starlike coronas. Within this model each coronal chain is confined to a virtual truncated cone, obtained by dividing the corona radially into f equal parts. The cone's wall set the blob size, $\xi(r)$, so that $\xi(r) \sim r/f^{1/2}$. The associated confinement free energy per chain, F_{corona}, is thus given by[12,13,15]

$$F_{corona}/kT \sim f^{-1}\int_{R_{core}}^{R_{core}+H} \xi^{-3}r^2\,dr \sim f^{1/2}\ln (R_{core} + H)/R_{core} \quad \text{(II.2i)}$$

where H is given by

$$H \sim f^{1/5}N_A^{3/5}a \quad \text{(II.2ii)}$$

where a denotes the typical monomer size in a flexible coil. (ii) The opposite limit obtains for $H \ll R_{core}$. In this case the coronal layers are essentially flat. The densely grafted coils are now pictured as stretched chains of blobs of size d; i.e., the chains are confined to virtual cylindrical capillaries of diameter d. The coronal free energy per chain is thus[10]

$$F_{corona}/kT \sim H/d \sim N_A(a/d)^{5/3} \quad \text{(II.3i)}$$

where H is given by

$$H \sim N_A(a/d)^{2/3}a \quad \text{(II.3ii)}$$

As noted earlier there is no penalty term associated with the deformation of core blocks in micelles formed by rod-coil copolymers. Accordingly, the total free energy per aggregated chain is given by

$$F = F_{interface} + F_{corona} \quad \text{(II.4)}$$

The aggregate equilibrium structure corresponds to a min-

imum in F; i.e., $\partial F/\partial f = 0$. For starlike micelles, $H \gg R_{core}$, we may write F as

$$F/kT \sim (\gamma d^2/kT)(L/d)f^{-1/2} + f^{1/2} \quad \text{(II.5)}$$

where terms linear in f are omitted and the logarithmic factor in F_{corona} is approximated as constant. The equilibrium condition then yields

$$f \sim (\gamma d^2/kT)L/d \sim N_B \quad \text{(II.6)}$$

where L is taken to scale linearly in N_B, $L \sim N_B$. Accordingly

$$R_{core} \sim (\gamma d^2/kT)^{1/2}(L/d)^{1/2} \sim N_B^{1/2} \quad \text{(II.7i)}$$

$$H \sim N_B^{1/5} N_A^{3/5} a \quad \text{(II.7ii)}$$

This regime obtains for $H \gg R_{core}$ providing that $L > 2H$ to avoid overlap of the coronal mops. Equation II.7 indicates that these requirements are met for

$$N_B^{4/3} \gg N_A \gg N_B^{1/2} \quad \text{(II.8)}$$

The flat corona regime obtains for $N_A < N_B^{1/2}$. F_{corona} is given by eq II.2ii and is independent of f. The equilibrium condition in this limit yields $f^{-3/2} = 0$, indicating a tendency to form lamellae ($f = \infty$). Our analysis suggests that the only stable micelles formed by rod–coil copolymers are endowed with starlike coronas. This conclusion justifies our initial claim regarding the irrelevance of rod tilt to micellar systems. Rod tilt increases the average separation of grafting sites, thus lowering F_{corona}. However, the effect on F_{corona} of starlike coronas is logarithmic and thus negligible.

A comparison to coil–coil micelles is helpful at this point. Coil–coil copolymers, as coil–rod copolymers, can form starlike micelles.[12] Clearly, these have a single corona instead of the two coronal mops found in rod–coil micelles. The functional form of F_{corona} is identical in the two systems. However, differences in core geometry result in dissimilar expressions for $F_{interface}$. In coil–coil micelles the core is spherical, consisting of f flexible grafted coils in a meltlike state. The core volume is thus proportional to $fN_B a^3$. As a result, $F_{interface} \approx f^{-1}\gamma R_{core}^2 \sim f^{-1/3}N_B^{2/3}$ rather than $F_{interface} \approx f^{-1}\gamma R_{core}L \sim f^{-1/2}dL$ in rod–coil micelles. As a result, $f \sim N_B^{4/5}$ in coil–coil starlike micelles as opposed to $f \sim N_B$ in rod–coil starlike micelles. Also, coil–coil copolymers, as opposed to coil–rod copolymers, can form "crew cut" micelles endowed with shallow, essentially flat, coronas. In these micelles $F_{interface}$ is balanced by the deformation free energy of the flexible core blocks. The absence of a similar term in rod–coil "crew cut" micelles diminishes their thermodynamical stability.

III. Lamellar Sheets

To bring out the distinctive features of rod–coil lamellae, we adopt a highly simplified model. Following de Gennes,[8] we consider a single flat sheet in a lamellar phase, assuming absence of direct overlap between the sheets. Fluctuations effects, curvature energies, etc., are ignored.[16] The core model used in section II is retained, but rod tilt is now allowed, i.e., the rods are aligned and their tips toe the basal planes, but their axes can be tilted with respect to the lamellar axis. As for micelles, the lamella's equilibrium structure is determined by the interplay of F_{corona} and $F_{interface}$. However, the lamellar geometry imposes important modifications on the argument: (i) The lateral, edge contribution to $F_{interface}$ is negligible for lamellae. (ii) The lamellar coronas are, in effect, *flat* grafted layers ($H \ll R_{core}$). As a result, rod tilt assumes

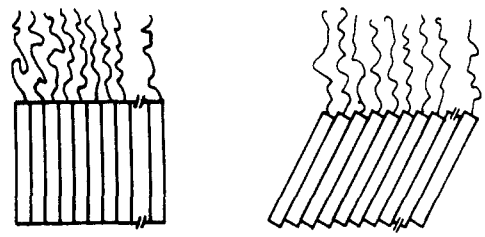

Figure 3. Schematic cross section in rod–coil lamella exhibiting a tilting, smectic A–smectic C transition. The lamellar core consists of immiscible aligned rods. The "corona" is, in effect, a flat grafted layer. When the surface free energy is dominant the untilted, smectic A, state is expected. The tilted, smectic C, state obtains when the deformation free energy of the grafted coils is large enough.

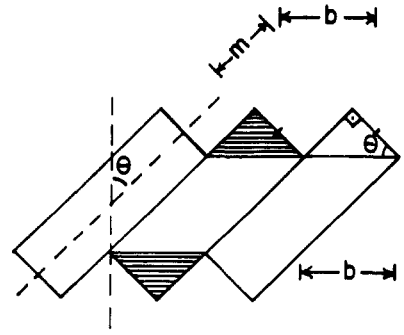

Figure 4. Detailed cross section of a tilted, smectic C, lamellar sheet. The rods, of length L and diameter d, are tilted at angle θ with respect to the normal. The distance between grafting sites, in the tilt plane, is denoted by b. The tilt exposes part of the rods lateral surface (lined). The area of the exposed surface equals the lateral surface area of a right circular cylinder of height m and diameter d.

crucial importance: Rod tilt increases the separation between grafting sites, thus lowering F_{corona}. At the same time it increases the core surface area and the associated $F_{interface}$. The competition between these two terms gives rise to a first-order tilting transition in this system[5] (Figure 3).

In the absence of tilt, $\theta = 0$, only the rods' bases are exposed to the solvent. The associated free energy per rod is thus $F_{interface} \sim \gamma d^2$. An increase in the tilt angle results in partial exposure of the rod lateral surface. The area of the newly exposed surface equals the lateral surface area of a right circular cylinder of diameter d and height m (Figure 4). As $m = d|\tan\theta|$, the corresponding surface contribution to F is $F_{interface} \sim \gamma d^2(1 + |\tan\theta|)$. The tilt also results in a lower grafting density. While d remains the shortest distance between grafting sites, the largest separation is now $b = d/\cos\theta$. The modified coronal term is accordingly $F_{corona}/kT \sim N_A(a^2/bd)^{5/6} \sim N_A(a/d)^{5/3}\cos^{5/6}\theta$ rather than $N_A(a/d)^{5/3}$. Altogether F is given by

$$F/kT \sim (\gamma d^2/kT)(1 + |\tan\theta|) + N_A(a/d)^{5/3}\cos^{5/6}\theta \quad \text{(III.1)}$$

$$F/kT \sim \gamma d^2/kT + N_A(a/d)^{5/3}\hat{F}(\delta,\theta) = \gamma d^2/kT + N_A(a/d)^{5/3}(\delta|\tan\theta| + \cos^{5/6}\theta) \quad \text{(III.1i)}$$

where δ is defined as

$$\delta = (\gamma d^2/kT)N_A^{-1}(a/d)^{-5/3} \quad \text{(III.2)}$$

δ is the ratio of $F_{interface}$ and F_{corona} in the absence of tilt, $\delta = F_{interface}(\theta=0)/F_{corona}(\theta=0)$. Clearly, no tilt is expected for $\delta > 1$. As δ is lowered, tilt becomes beneficial as a way of lowering F_{corona}. However, for low tilt angles, $\theta \ll 1$, the associated increase in $F_{interface}$ is dominant. This

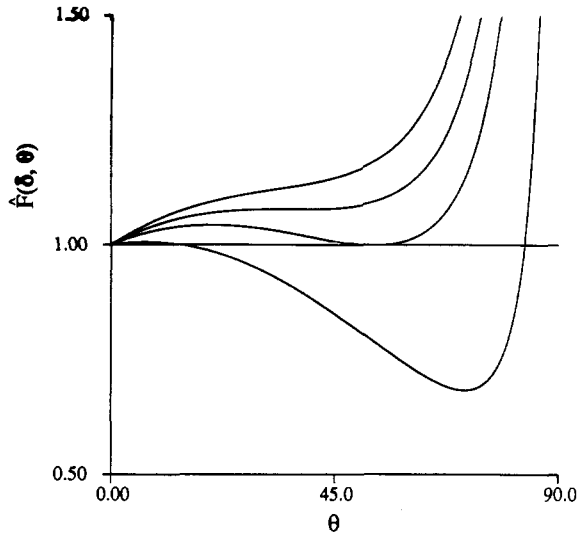

Figure 5. Plots of $\hat{F}(\delta,\theta) = \delta \tan\theta + \cos^{5/6}\theta$ vs θ for $\delta = 0.4$, $\delta_{infl} = 0.332$, $\delta_{trans} = 0.26$, and $\delta = 0.1$.

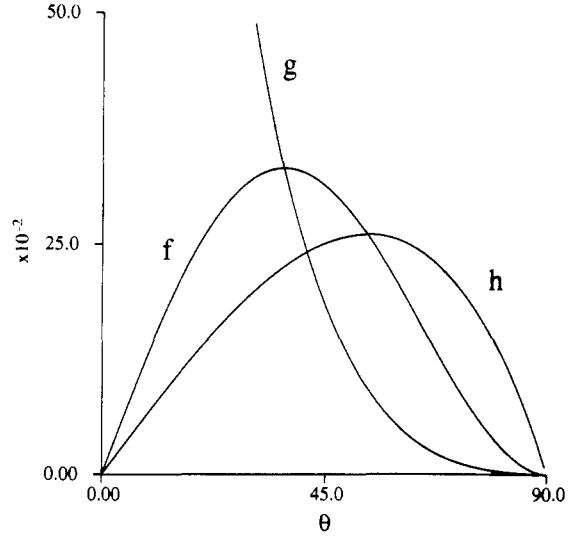

Figure 6. Graphical solution of $f(\theta) = g(\theta)$ corresponding to $\partial F/\partial\theta = \partial^2 F/\partial\theta^2 = 0$ and of $f(\theta) = h(\theta)$, corresponding to $F(\delta_{trans},\theta_{trans}) = F(\delta_{trans},0)$ and $\partial F/\partial\theta = 0$.

is easily seen since for $\theta \ll 1$ $F_{interface}/kT \sim (\gamma d^2/kT)(1 + \theta)$ while $F_{corona}/kT \sim N_A(a/d)^{5/3}(1 - \theta^2)$. As a result F develops an unstable region and the tilt occurs via a first-order phase transition (Figure 5). A stable tilted phase occurs for δ values such that $\partial F/\partial\theta = 0$, $\partial^2 F/\partial\theta^2 > 0$, and $F(\delta,\theta=0) > F(\delta,\theta)$. The equilibrium condition, $\partial F/\partial\theta = 0$ leads to

$$\delta = f(\theta) \equiv (5/6)\cos^{11/6}\theta \sin\theta \qquad \text{(III.3)}$$

For $\delta > 0.3321$ F is a monotonously increasing function and eq III.3 has no roots (Figure 6). F exhibits an inflection point for $\partial^2 F/\partial\theta^2 = \partial F/\partial\theta = 0$ where $\partial^2 F/\partial\theta^2 = 0$ is equivalent to

$$\delta = g(\theta) \equiv (5/72)\cot\theta \cos^{5/6}\theta(1 + 5\cos^2\theta) \qquad \text{(III.4)}$$

The inflection point occurs for $\delta_{infl} = 0.332$ and $\theta_{infl} = 36.45°$. This also specifies the single solution of eq III.3 for δ_{infl}. For $\delta < \delta_{infl}$, F develops a second minimum located at $\theta > 36.45°$. In this regime eq III.3 has two roots. The physical solution, corresponding to the second minimum, obeys the stability condition $\partial^2 F/\partial\theta^2 > 0$. The tilted phase is truly stable when its free energy per chain, $F(\delta_{trans},\theta_{trans})$ equals that of the untilted lamella, $F(\delta_{trans},\theta=0)$, i.e., when eq III.3 is supplemented by the condition

$$\delta = h(\theta) \equiv (1 - \cos^{5/6}\theta)\cot\theta \qquad \text{(III.5)}$$

This condition obtains for $\delta_{trans} = 0.26$ and $\theta_{trans} = 53.30°$ (Figure 6). In line with common practice we consider lamellar states between δ_{infl} and δ_{trans} metastable. The phase transition is said to occur at δ_{trans}: the lamellar thickness is expected to undergo a sharp transition. For $\delta > \delta_{trans}$ the core and coronal thicknesses are given by

$$H_{core} \approx L \sim N_B \qquad \text{(III.6)}$$

$$H_{corona} \sim N_A(a/d)^{2/3} \qquad \text{(III.7)}$$

while for $\delta < \delta_{trans}$ and $\theta > \theta_{trans}$ we expect

$$H_{core} \approx L\cos\theta \sim N_B\cos\theta \qquad \text{(III.8)}$$

$$H_{corona} \sim N_A(a^2/bd)^{1/3} \sim N_A(a/d)^{2/3}\cos^{1/3}\theta \qquad \text{(III.9)}$$

θ's δ dependence is determined by eq III.3. For $\pi/2 - \theta \ll 1$ it yields $\theta \approx \pi/2 - (6/5)^{6/11}\delta^{6/11}$. A numerical fit leads to the following expression for $\theta(\delta)$ in the range $\delta_{trans} > \delta > 0$ (Figure 7)

$$\theta \approx 1.57 - 1.23\delta^{0.58} - 12.1\delta^{3.73} \qquad \text{(III.10)}$$

This description fails for $\delta \approx \pi/2$. In the vicinity of $\theta = \arctan(L/d)$ the lamellae, within this model, break down, and our discussion is no longer meaningful. Tilt angles greater than $\arccos(d/R_F)$, where R_F is the Flory radius of the A coil, are also meaningless. In this case the coils no longer overlap in the tilt plane and there is no driving force for further increase in θ.

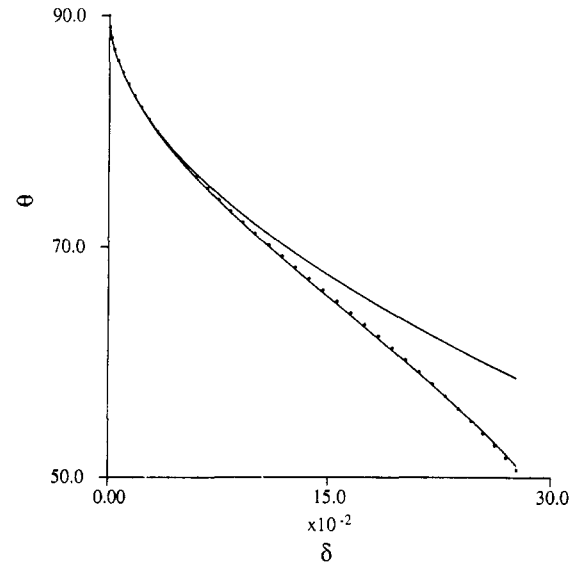

Figure 7. Plot of $\theta(\delta)$ vs δ in the range $\delta_{trans} < \delta < 0$. The upper curve corresponds to the asymptotic solution $\theta = \pi/2 - (6/5)^{6/11}\delta^{6/11}$. The lower curve describes the full numerical solution for $\theta(\delta)$ while the points are given by the numerical fit (eq III.10).

As noted earlier, the B rods are, in effect, grafted to the core–solvent interface. The tilting transition occurs because the grafted rods are also coupled to the densely grafted, strongly stretched A coils. Our discussion thus complements existing treatments of grafted rods' phase behavior[17-20] where the phase transitions are solely due to rod–rod and rod–surface interactions. Coil–coil lamellae provide another reference system of interest. No phase transitions are expected in this case. A simple analysis of this system[8] begins with a free energy per chain, F, given by $F = F_{core} + F_{interface} + F_{corona}$. The core is now modeled as a melt of grafted, flexible blocks. The combination of grafting and constant density constraints leads

to stretching of the core blocks. The corresponding penalty term, F_{core}, is given by $F_{core} \approx R_0^2/L_{core}^2 \sim N_B a^2/L_{core}^2$ where L_{core} is the thickness of the core layer. Apart from the role of F_{core}, this system differs from rod–coil lamellae in that the average separation between grafting sites, D, is isotropic in the grafting plane. Furthermore, D uniquely defines the surface area per chain $\sigma = D^2$. The coil–coil lamellae exhibit two regimes. In one $F_{interface}$ is primarily balanced by F_{corona}. In the second, the dominant penalty term is F_{core}. A smooth crossover between the two regimes occurs as the relative size of the two blocks is varied. Finally, our results should be considered from the view point of liquid-crystal research. As noted in the introduction, rod–coil copolymers are the macromolecular counterpart of monomeric smectogens. However, these polymeric smectogens, as opposed to their monomeric analogues, are also surfactants capable of forming smectic liquid-crystalline phases in solution. This is an important advantage since the analysis of swollen lamellar phases, when individual sheets are nonoverlapping, is exceptionally simple. In particular, our analysis suggests a simple physical origin to the tilting, smectic A–smectic C, phase transition[4,21] in rod–coil lamellae. This result is of interest as this system is directly related to melt lamellar phases and to thermotropic smectic phases formed by monomeric mesogens.

IV. Design of Ferroelectric Lamellae and Paraelectric Micelles

An elegant molecular design for ferroelectric liquid crystals was recently suggested by Petschek and Wiefling (PW).[6] Their design utilizes ABC triblock copolymers in which the middle, B, segment is a rigid mesogenic block endowed with a dipole moment $\mu \sim N_B$. The incompatibility of the flexible A and C coils is used to align the dipoles of the B blocks. The original discussion of this scheme focused on thermotropic, ferroelectric, smectic liquid crystals, i.e., on melt lamellar mesophases exhibiting spontaneous polarization. Unfortunately such polymeric melts are highly viscous. This is a serious deficiency since the interest in ferroelectric liquid crystals is due, in part, to their potential as a fast-working medium for electrooptic devices. In particular, the melt viscosity may counteract the effect of ferroelectric order, yielding samples with slow switching rates. One may avoid this difficulty by using micelles formed by appropriate ABC triblock copolymers in a selective solvent of low molecular weight. Microphase separation in the micellar corona[22] can be used to align the dipoles in the micellar core (Figure 8). The micellar solutions thus formed combine three desirable properties: (i) optical activity due to liquid crystalline micellar cores; (ii) paraelectricity, possibly superparaelectricity, due to the alignment of the core dipoles; (iii) low viscosity characteristics of low molecular weight solvents. Such solutions are reminiscent of liquid-crystalline "emulsions". Their response times are expected to be short because of their combined paraelectricity and low viscosity.

Before we proceed to discuss the design of such paraelectric micelles, it is helpful to present the PW argument in a modified form. We focus on ferroelectric order in lamellar, smectic phases formed by ABC triblock copolymers with flexible blocks of equal size; i.e., $N_A = N_C$. The aggregation takes place in a highly selective solvent of low moleclar weight. It is a poor solvent for the mesogenic B blocks and an equally good solvent for both A and C coils. Again, the lamellar phase considered is highly swollen so that adjacent sheets are essentially nonoverlapping. We may thus focus on the ferroelectric alignment in a single sheet (Figure 9). Electrostatic interactions between lamellae are ignored. For simplicity we confine our discussion to the high "surface tension" limit, $\gamma d^2 \gg \mu^2/d^3$ and $\gamma d^2 \gg kTN_A(a/d)^{5/3}$, for which smectic A is the only stable phase. Our discussion is founded on the observation that each copolymer is endowed with two dipoles: an electric dipole μ and a "chemical dipole" due to the dissimilarity of the A and C blocks. The PW method requires ABC copolymers synthesized so that the two dipoles are consistently aligned. In other words, the vector joining the AB and BC junctions is always parallel (or antiparallel) to μ. The electrical and the chemical dipoles are mutually noninteracting, but each electric dipole is rigidly coupled to the associated chemical dipole. The flat lamellar sheet considered is thus analogous to a two-dimensional Ising lattice with sites occupied by combined electrical and chemical dipoles. The interaction between electrical dipoles promotes antiferroelectric order, i.e., formation of antiparallel dipole dimers. The chemical dipoles, on the other hand, favor parallel, ferroelectric alignment, since it minimizes the number of contacts between the incompatible A and C monomers. It is thus possible to tune the interaction parameter between such combined dipoles by adjusting the relative size of the flexible coils ($N_A = N_C$) and the rigid B blocks (N_B). An explicit expression for F, the free energy per copolymer, is needed to make this discussion more

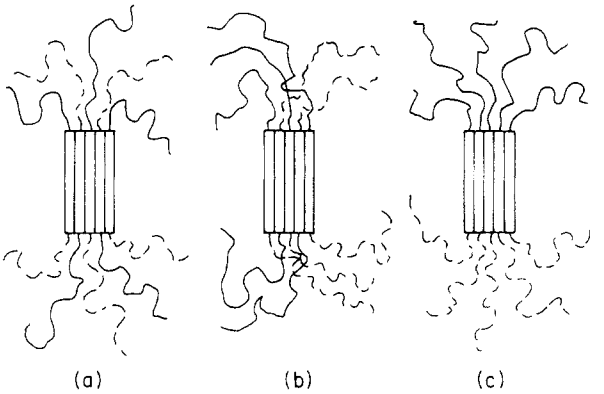

Figure 8. Microphase separation in ABC coil–rod–coil micelles having two outcomes. The uniformly mixed, randomly aligned micelle (a) may demix by intracoronal process: The coronal mops retain their overall composition but separate into A (continuous) and C (broken) rich domains (b). When the domains' boundary free energy is high enough the intercoronal process dominates (c). It yields coronal mops, which are rich in either A or C. When the rod blocks carry an electrical dipole pointing from A to C, the intercoronal microphase separation results in aligned core dipoles leading to paraelectric micelles.

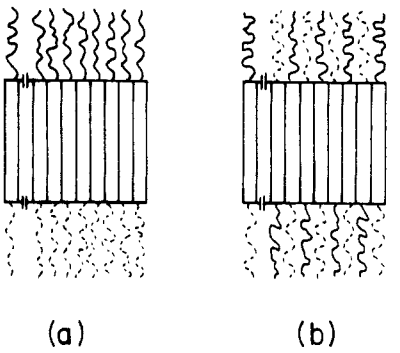

Figure 9. Schematic cross section in an ABC coil–rod–coil lamella. When the interaction parameter between the chemical dipoles, the AC incompatibility, is strong enough, both chemical and electrical dipoles align (a). In the opposite case the system may exhibit antiferroelectric order or random alignment (b).

concrete. Such an expression is easily obtained in the framework of the Braggs–Williams approach to the Ising model.[23] In the regime of interest, where rod tilt is irrelevant, the mean fraction of upward pointing dipoles, x, is the variable of interest. As is customary, we express F in terms of $\Delta = 2x - 1$, the deviation from $x = 1/2$. Three Δ-dependent terms appear in F: Interactions between the electrical dipoles give rise, within the Braggs–Williams approximation, to $E_{dipole} = -(\epsilon/2)\Delta^2$ where $\epsilon \sim -\mu^2 j/d^3$ is the dipole–dipole interaction parameter and j is the coordination number. This interaction energy must be supplemented by a term accounting for the up–down orientational entropy of the rods, $S/k = -[(1 + \Delta)/2] \ln [(1 + \Delta)/2] - [(1 - \Delta)/2] \ln [(1 - \Delta)/2]$. Because of the definite, rigid coupling between the electrical and chemical dipoles, this term also accounts for the lateral AC mixing entropy per grafted chain. The AC mixing energy per coil gives rise to $E_{mix}/kT = (\hat{\chi}/2)(1 - \Delta^2)$ where $\hat{\chi}$ is the interaction parameter between the grafted A and C coils.[24] Altogether we have $F = F_o + E_{dipole} + E_{mix} - kTS$ where Δ-independent terms are grouped in F_o. These include the interfacial term, γd^2, and the deformation free energy per grafted coil, $N_A(a/d)^{5/3}kT$. F is thus given by

$$F/kT = F_o/kT - (\epsilon/2kT)\Delta^2 + (\hat{\chi}/2)(1 - \Delta^2) + [(1 + \Delta)/2] \ln [(1 + \Delta)/2] + [(1 - \Delta)/2] \ln [(1 - \Delta)/2] \quad \text{(IV.1)}$$

Minimization with respect to Δ yields

$$\Delta = \tanh\left(\frac{\epsilon + \hat{\chi}}{kT}\Delta\right) \quad \text{(IV.2)}$$

In the absence of a chemical dipole, when A and C are indistinguishable and $\hat{\chi} = 0$, eq IV.2 reduces to the result obtained for the bare Ising lattice. In our system $\hat{\chi}$ is positive and rather large, scaling as $\hat{\chi} \sim N_A(a/d)^{2.03}$. This is an important point since ϵ, in our case, is negative. Consequently, the bare electric dipoles should exhibit random orientations ($|\epsilon/kT| \ll 1$) or antiferroelectric order ($|\epsilon/kT| \gg 1$). The combined electrical–chemical dipoles may, on the other hand, exhibit ferroelectric order since their interaction parameter $\hat{\epsilon} = \epsilon + \hat{\chi}$ is positive for large enough $\hat{\chi}$. In particular, because $\epsilon \sim N_B^2$ and $\hat{\chi} \sim N_A$, it is possible to adjust the size of the two blocks so that $\hat{\chi}$ is sufficiently large to ensure a positive $\hat{\epsilon}$. A stable ferroelectric phase is expected below T_c given by $kT_c = \hat{\epsilon}$.

How applicable are the above considerations to micelles formed by ABC coil–rod–coil copolymers? The broad features of our discussion remain valid, but certain modifications are necessary because of the micelles' finite size. While an abrupt alignment is still expected, a proper phase transition is ruled out since the system is no longer infinite. It is also necessary to account for electrostatic edge effects. Apart from these two points, one must allow for the special features of microphase separation in micelles.[22] In our case, it can take two routes (Figure 8): (i) Intercoronal microphase separation involving AC exchange between the two coronal mops is one. This process requires flips of the chemical dipoles and is thus analogous to the lamellar process considered above. It is also the process of interest as it results in alignment of the electrical dipoles. (ii) Intracoronal microphase separation is possible as well. In it the A and C coils undergo demixing transition within each coronal mop. The orientation of the chemical dipoles and the overall composition of each coronal mop are retained. The small micellar size and the starlike coronal structure allow for coronal microphase separation with no lateral rearrangement of the B dipoles, a process with no clear counterpart in lamellae. Clearly, in this system intermicellar exchange is thermodynamically immaterial. The overall micellar composition is thus constant, consisting of an equal number of A and C blocks. To determine the equilibrium structure of demixed micelles it is necessary to compare the free energy per chain following the two processes. A simple discussion of these effects is possible in the following situation: A micellar solution is deeply quenched so as to cause complete AC demixing. Initially all coronal mops are uniformly mixed comprising an equal number of A and C blocks. The intramicellar process results in partitioning each corona into two equal hemispherical domains consisting exclusively of A or C blocks. Providing the quenched state is far removed from the critical point, the coronal dimensions are large in comparison to the relevant correlation length, and a sharp domain boundary is expected. When the associated boundary free energy is high enough the intermicellar process yields a state of lower free energy. F as given by eq IV.1 provides a basis for a more quantitative description. However, F should be modified by replacing $E_{mix} = \hat{\chi}(1 - \Delta^2)$ by $E_{line} = f^{-1}\tau L(\Delta)$ where $L(\Delta)$ is the overall length of the boundary between the A and C rich domains and τ is the associated "line tension".[25] This modification is required since the transition is now driven by line tension rather than interactions between chemical dipoles. We focus on the limit where dipole interactions and the mixing free energy are sufficiently small so that the equilibrium micellar structure of section II is retained. For simplicity the coronal blocks are assumed to be grafted onto a sphere of radius R_{core}. Since the dimensions of starlike coronas are much larger than R_{core}, the precise geometry of the supporting surface is unimportant. This assumption is convenient because it leads to a simple expression for the boundary length:[22] $L(\Delta) = P_{core}(1 - \Delta^2)^{1/2}$ where $P_{core} = 2\pi R_{core}$ is the perimeter of the sphere. Altogether we have

$$F/kT = F_o/kT - (\epsilon/2kT)\Delta^2 + (\tau P_{core}/fkT)(1 - \Delta^2)^{1/2} + \frac{1 + \Delta}{2} \ln \frac{1 + \Delta}{2} + \frac{1 - \Delta}{2} \ln \frac{1 - \Delta}{2} \quad \text{(IV.3)}$$

The qualitative behavior of ABC micelles is reflected in this F. However, precise correspondence is not to be expected since this choice of F does not account for the small micellar size. For example, while F as given is appropriate for lamellae, E_{line} may only drive the alignment in micelles. Also, the treatment of Δ as a continuous variable is questionable. Because of these considerations we avoid a thorough analysis of F. The minimization of F yields

$$\Delta = \tanh\left[\frac{|\epsilon|}{kT}(-\Delta + \alpha\Delta(1 - \Delta^2)^{-1/2})\right] \quad \text{(IV.4)}$$

where α is given by

$$\alpha = \tau P_{core}/f|\epsilon| \quad \text{(IV.5)}$$

Evidently, eq IV.4 is solved by $\Delta = 0$ and by $\Delta = \pm 1$. $\Delta = 0$ corresponds to the state formed by the intercoronal process. $\Delta = \pm 1$ obtains for a perfectly aligned state due to intercoronal microphase separation. Actually, while the roots $\Delta = \pm 1$ satisfy eq IV.4, $\partial F/\partial\Delta$ diverges at these points. Yet, these solutions correspond to true minima in F. When $\Delta = 0, \pm 1$ are all minima, eq IV.4 has two extra roots at $\Delta = \pm|\Delta_m|$ such that $1 > |\Delta_m| > 0$. These two symmetrical solutions specify the location of free-

energy maxima. The minimum at $\Delta = 0$ occurs whenever $f^{-1}\tau P_{core} < kT + |\epsilon|$ or $\alpha < 1 + kT/|\epsilon|$. The two minima attain equal depth for $f^{-1}\tau P_{core} - (kT \ln 2) = |\epsilon|$ or $\alpha = (kT \ln 2)/|\epsilon| + 1/2$. For sufficiently large α values, when the boundary free energy more than compensates for the orientational entropy and the dipolar interactions, paraelectric micelles are expected. Clearly, α increases with the polymerization degrees of the flexible blocks, $N_A = N_C$. α's precise N_A dependence is determined by the scaling behavior of τ, P_{core}, f, and $|\epsilon|$. $|\epsilon|$ was assumed to scale as N_B^2. In the present case, where the micelles are assumed to retain the equilibrium structure of section II, we have $P_{core} \sim N_B^{1/2}$ and $f \sim N_B$. The scaling behavior of τ is more difficult to obtain. For a flat grafted layer, as exemplified by the corona of untilted rod–coil lamella, one finds[22] $\tau/kT \sim N_A^{1/3}/d^{8/9}$. However, the argument leading to this expression relies on the Alexander model, which is not applicable to spherical grafted layers. While a similar trend is expected in our case, the dependence on N_A and especially on d should be weaker.

V. Discussion

The equilibrium structures of rod–coil and coil–coil aggregates are significantly different. The micellar geometry and scaling behavior are dissimilar. Also, different scaling laws and phase behavior characterize the two lamellar types. The differences are due to the distinctive properties of rodlike blocks: (i) The configuration of rigid, rodlike polymers is unique. Consequently no deformation occurs upon aggregation, and the corresponding penalty term is absent. (ii) Immiscible rodlike blocks tend to pack with their axes aligned and their tips toeing a single plane so as to minimize their surface free energy. The core geometry is thus different from that of coil–coil aggregates.

Apart from current interest in the aggregation behavior of polymeric surfactants, this problem is also relevant to liquid-crystal research. Rod–coil copolymers provide a polymeric model for monomeric smectogens. The analysis of the polymeric system is typically simpler. This is illustrated by the simple picture of the physical origin of the smectic A–smectic C transition in rod–coil lamellae. Also, ABC coil–rod–coil copolymers afford opportunities for the design of ferroelectric or paraelectric working media for electrooptic devices. Finally, the interest in the rich phase behavior of surfactant monolayers motivated the study of mobile grafted rods. In these discussions the rods may be thought of as anchored surfactants in an all-trans configuration, and their phase behavior is determined by rod–rod and rod–surface interactions. Rod–coil copolymers may be considered as surfactants having a segment in an all-trans configuration. Accordingly the tilting transition found in rod–coil lamellae may shed some light on the phase behavior of surfactant monolayers. It is especially interesting since the transition is due to rod–coil coupling rather than to rod–rod or rod–surface interactions.

Existing experimental studies of coil–rod block copolymers deal mostly with copolymers incorporating polypeptide blocks. These investigations, largely pursued by Douy and Gallot,[3] are motivated by two arguments: (i) Rod–coil copolymers containing polypeptide blocks may serve as model system for structural proteins in biological membranes. (ii) The variety of conformations exhibited by polypeptide chains is expected to yield novel copolymers of technological interest. Experimental reasons and the interest in membranes directed these studies toward lamellar phases formed by AB coil–rod and ABA coil–rod–coil block copolymers. Little attention was given to micelles formed by these polymeric surfactants or to the aggregation behavior of ABC coil–rod–coil copolymers. While copolymers incorporating polypeptide blocks are of interest, the study of rod–coil copolymers requires a simpler model system. The polypeptides' rich configurational repertoire is a deficiency as well as an advantage. In particular, polypeptide blocks can fold rather than tilt. These two options may compete or coexist, thus making for difficulties in interpretation. Rod–coil copolymers based on rigid synthetic polymers, preferably main-chain mesogens, are better suited as model systems. AB coil–rod or ABA coil–rod–coil copolymers are equally suitable for the study of the aggregates equilibrium structure: The two species should form aggregates exhibiting identical scaling behavior. The route to paraelectric micelles depends on the synthesis of ABC coil–rod–coil copolymers such that the electrical dipole is consistently aligned with the chemical dipole. However, in view of the crucial role of microphase separation in this scheme it is worthwhile to study demixing in more accessible systems. In particular, one may utilize mixed micelles formed by AB and CB coil–rod copolymers. The demixing behavior in such systems is somewhat different since the overall micellar composition may change because of intermicellar exchange. Yet, such experiments yield relevant information while avoiding the more difficult synthesis of ABC triblock copolymers. Similar considerations apply to the implementation of the Petschek–Wiefling scheme to lamellar systems.

Acknowledgment. It is a pleasure to acknowledge helpful discussions with S. Alexander and P.-G. de Gennes. D. Davidov acquainted me with ref 6. This research was supported by the U.S.–Israel Binational Science Foundation (BSF), Jerusalem, Israel. The Fritz Haber Research Center is supported by the Minerva Gesellschaft für die Forschung, mbH, Munich, BRD.

References and Notes

(1) Dowell, F. *Phys. Rev. A* **1983**, *28*, 3520, 3526.
(2) Semenov, A. N.; Vasilenko, S. V. *Sov. Phys.-JETP* (*Engl. Transl.*) **1986**, *63*, 70.
(3) (a) Douy, A.; Gallot, B. *Polymer* **1987**, *28*, 147 and references therein. (b) Nakajima, A.; Hayashi, T.; Kugo, K.; Shinoda, K. *Macromolecules* **1977**, *12*, 480.
(4) de Gennes, P.-G. *The Physics of Liquid Crystals*; Clarendon Press: Oxford, 1974.
(5) Halperin, A. *Europhys. Lett.* **1989**, *10*, 549.
(6) Petschek, R. G.; Wiefling, K. M. *Phys. Rev. Lett.* **1987**, *59*, 343.
(7) de Gennes, P.-G.; Taupin, C. J. *Phys. Chem.* **1982**, *86*, 2294.
(8) de Gennes, P.-G. In *Solid State Physics*; Leibert, L., Ed.; Academic Press: New York, 1974; Supplement 14.
(9) This terminology was designed and is most appropriate for spherical micelles formed by diblock copolymers. For brevity we use these terms in the wider sense indicated in the text.
(10) Alexander, S. *J. Phys.* (*Les Ulis, Fr.*) **1977**, *38*, 983.
(11) A rigorous analysis of the aggregation behavior should utilize a grand canonical free energy, allowing for all possible mesophases, polydispersity, fluctuation, etc. For simplicity we utilize the Shulman approximation[7] in which the free energy per aggregated chain is used and a single aggregate type is considered. This approach also does not allow for the role of the chemical potential in determining the aggregate's structure. Also, it does not provide a basis for a complete discussion of the system's phase behavior. For example, the relative stability of the lamellar and micellar phases is not obtainable by this approach.
(12) Halperin, A. *Macromolecules* **1987**, *22*, 1943.
(13) Marques, C.; Joanny, J. F.; Leibler, L. *Macromolecules* **1988**, *21*, 1051.
(14) Daoud, M.; Cotton, J. P. *J. Phys.* (*Les Ulis, Fr.*) **1982**, *43*, 531.
(15) Witten, T.; Pincus, P. A. *Macromolecules* **1986**, *19*, 2509.
(16) These requirements imply $\gamma d^2 \gg kT$.

(17) Halperin, A.; Alexander, S.; Schechter, I. *J. Chem. Phys.* **1987**, *86*, 6550; **1989**, *61*, 1383.
(18) Chen, Z.-Y.; Talbot, J.; Gelbart, W. M.; Ben-Shaul, A. *Phys. Rev. A* **1988**, *61*, 1376.
(19) Wang, Z.-G. *J. Phys.* (*Les Ulis, Fr.*), in press.
(20) Moore, B. G. *J. Chem. Phys.* **1989**, *91*, 1381.
(21) Prost, J. *Adv. Phys.* **1984**, *33*, 1.
(22) Halperin, A. *J. Phys.* (*Les Ulis, Fr.*) **1988**, *49*, 131.
(23) Huang, K. *Statistical Mechanics*; John Wiley: New York, 1987.
(24) Halperin, A. *Europhys. Lett.* **1987**, *4*, 439. The blob argument in this paper suggests that the interaction parameter between densely grated A and C coils scales as $\hat{\chi} \sim N_{blob}\chi_{pp}^{blob} \sim N_Z(a/d)^{5/3}\chi_{pp}^{blob}$ where N_{blob} is the number of blobs per chain and χ_{pp}^{blob} is the interaction parameter between A and C blobs. The final result of this paper follows from the assumption $\chi_{pp}^{blob} \approx \chi_{pp}$ where χ_{pp} is the corresponding monomer-monomer interaction parameter. A more rigorous analysis (Broseta, D.; Leibler, L.; Joanny, J. F. *Macromolecules* **1987**, *20*, 1935) suggests $\chi_{pp}^{blob} \sim \chi_{pp}\phi\chi^{SD}$ where $\chi^{SD} \approx 0.275$, thus leading to the result quoted in the text.
(25) Properly speaking, the term "line tension" refers to the free energy per unit length associated with the three-phase boundary. See, for example: Rowlinson, J. S.; Widom, B. *Molecular Theory of Capillarity*; Clarendon Press: Oxford, 1982. For convenience we use this term for the two-dimensional analogue of surface tension.

Fluorescence Probing of Microdomains in Aqueous Solutions of Polysoaps. 2. Study of the Size of the Microdomains

W. Binana-Limbelé and R. Zana*

Institut Charles Sadron (CRM-EAHP), CNRS-ULP Strasbourg 6, rue Boussingault 67083 Strasbourg Cedex, France

Received July 21, 1989; Revised Manuscript Received November 15, 1989

ABSTRACT: The time-resolved fluorescence quenching method has been used to investigate the size (number of repeat units) of microdomains in solutions of poly(disodium maleate-*co*-decylvinylether) and poly(disodium maleate-*co*-hexadecyl vinyl ether) referred to as PS10 and PS16, using pyrene as the fluorescence probe and the dodecylpyridinium ion as the quencher. The shape of the decay curves reveals that the microdomains are somewhat polydisperse in size. In the case of PS10 the number of repeat units per microdomain was found to decrease nearly linearly upon increasing the degree of neutralization of the maleic acid moieties. For PS10 the number of repeat units per microdomain is nearly independent of the polysoap concentration and polymerization degree as well as of the ionic strength and temperature. For PS16, the number of repeat units per microdomain is independent of the polymerization degree but increases much with temperature. Also, it is much larger than that for PS10. Moreover the decay data for PS16 suggest that probe and quencher can rapidly migrate from microdomain to microdomain, on the fluorescence time scale. Overall the results suggest that the formation of a microdomain involves a single polysoap molecule and that several microdomains can be formed from a single polysoap molecule of high molecular weight. Such microdomains are connected by polysoap segments that may be the cause of the probe and quencher migration observed in PS16 solutions and also in PS10 solutions at 60 °C. The migrating molecules would move along these fairly hydrophobic segments.

Introduction

The term polysoap refers to alkali-metal salts of the alternating copolymers poly(maleic acid-*co*-alkyl vinyl ether).[1,2] In aqueous solution polysoaps give rise to hydrophobic microdomains,[1-10] somewhat similar to the micelles existing in solutions of soaps or surfactants at a surfactant concentration above the critical micellization concentration.

In the first part in this series,[11] pyrene fluorescence was used to probe the conformational state of polysoaps, where the alkyl group was *n*-butyl, *n*-decyl, and *n*-hexadecyl (referred to as PS4, PS10, and PS16, respectively) as well as of polymethacrylic acid and poly(maleic acid-*co*-styrene) as a function of the neutralization degree of the carboxylic groups. The same technique was used to investigate the comicellization of PS4 and alkyltrimethylammonium halide surfactants as a function of the surfactant concentration and alkyl chain length. The results clearly showed that the hydrophobic microdomains disappear upon neutralization of PS4, polymethacrylic acid, and poly(maleic acid-*co*-styrene) but persist even at full neutralization in PS10 and PS16. A compact conformation of PS10 and PS16 in aqueous solution had been previously inferred by Pefferkorn et al. from diffusion, conductivity, and viscosity measurements.[9,10]

There has been thus far few attempts to determine the number of repeat units N_c involved in a polysoap microdomain. This information is indeed rather difficult to obtain by classical techniques because polysoaps combine the complexity of polyelectrolytes and surfactant micelles. Barbieri and Strauss[8] attempted to determine N_c from potentiometric titration data and thus obtained values of 19 and 13 for PS4 and PS5 samples, respectively, of polymerization degrees (DP) much larger than these N_c values. Time-resolved fluorescence quenching (TRFQ) was later used by Hsu and Strauss[12] to determine the value of N_c in acidic solutions (pH = 4) of a sample of PS6 of DP = 1700. The low value found for N_c, 24, indicated that a single polysoap molecule can give rise to many microdomains. A different conclusion was reached by Chu and Thomas,[13a] who determined the value of N_c in a fully neutralized solution of poly(dipotassium maleate-*co*-octadecene) of DP = 24 by TRFQ. The value of N_c was found to be equal to the DP, within the exper-

0024-9297/90/2223-2731$02.50/0